CFD4NRS WITH A FOCUS ON EXPERIMENTAL AND CMFD INVESTIGATIONS OF BUBBLY FLOWS

G. Yadigaroglu
Prof. em. of Nuclear Engineering, ETHZ
Senior Advisor, Thermal Hydraulics Laboratory, PSI

M. Simiano, R. Milenkovic, R. Zboray, F. De Cachard, B. Smith
Thermal Hydraulics Laboratory, PSI
D. Lakehal, *ASCOMP GmBH*
B. Sigg, *Nuclear Engineering Laboratory, ETHZ*

Abstract

The paper discusses first current computational trends related to reactor safety problems and developments needed, as well as the need for new kinds of much more detailed experimental data for the validation of the new methods and codes. The numerous bubbly flow experiments conducted during the last decade at PSI are then reviewed and put in perspective with regards to the needs of the analysts. The latest experiments produced first-of-a-kind sets of experimental data from bubbly plumes and jets. Some of these data were ensemble or phase averaged to filter large-scale meandering and oscillations or coherent structures and make the time-dependent small-scale effects and stress terms visible. The large data sets that have been created can be further mined to extract additional information for the two-phase flow analyst.

Introduction and background

The use of Computation Fluid Dynamics (CFD) methods has become an everyday activity in many industries and has already been applied to reactor safety problems. Computational *Multi*-Fluid Dynamics or CMFD [1] methods are emerging as a new, additional tool for the analysis of reactor safety problems. The CFD methods have reached a certain maturity and their application to reactor problems, although it requires certain skills, is only limited by the availability of computing power, as recent exercises have shown [2,3]. The commercial CFD codes, as well as many more specialized codes developed at national laboratories and universities have also reached a satisfactory level of robustness and performance. Recent European programmes have addressed the issues of validation of CFD methods and tools and of good practices in programming [3]. The classical CFD and the more recent CMFD methods and codes will need to be coupled to the classical system analysis codes to provide the necessary local detail or 3D behaviour, when needed.

The CFD and CMFD methods address the problems at a much more fundamental and less globally empirical way; for example information on the turbulence near the wall is used instead of a friction factor and a heat transfer coefficient. Consequently, they are expected to provide results more independent of the scale of the system. The scalability of results obtained in small or medium-size systems to the real reactor geometries will then be better justified. However, to properly validate the application of CFD methods and codes to very-large-scale computational domains such as a complex reactor containment building, there is also a need to produce detailed experimental data in *large-scale* facilities at a much more fundamental and basic level then before – for example, not simply establish the pressure history and main flow paths and fluxes of fluids but also get detailed information on the flow fields and on the level of turbulence. Examples of such data collection efforts are the PANDA tests within the international SETH programme [4,5,6] whose objectives were to study mixing and distribution of steam/air/He mixtures, the behaviour of plumes etc., in multidimensional, multi-compartment, "clean" geometries using extensive and sophisticated instrumentation, for example Particle Image Velocimetry (PIV). There is a proposed extension, SETH-II, of this program with experimental work in both the PANDA and the MISTRA facilities (at PSI and at the French CEA laboratories in Saclay, respectively). In this case the focus will be on containment phenomena such as the effects of mass sources, heat sources, heat sinks, steam condensation caused by "cold" containment walls and by containment coolers; spray systems, mixing following the sudden opening of hatches, etc. [7].

Cascades of Computational Multi-Fluid Dynamics (CMFD)

The next frontier is the improvement of the existing and the development of new CMFD methods [8-12]. In multi-phase flows, the existence of several length scales is the rule and much more prevalent than in single-phase flows, where typically one has to deal with two scales, the scale of the equipment and the fine scale of turbulence. In a typical two-phase flow example, bubbly flow, one has at least three length scales: the scale of the equipment, the scale of the bubble and the fine scale of turbulence. Such multi-phase problems should also be tackled with computations, methods and tools appropriate at a multiplicity of time/space scales as we [13,14], as well as other authors [12,15], have already noted in previous publications. Let us refer to these as the micro-, the meso- and the macro-scale. The entire system (say, the primary system of a reactor or the containment) can, for example, be modelled at the macro-scale; a system component may need to be examined at the meso-scale. Local flow in a critical part of a component may need to be addressed at the micro-scale. At each level of the scale hierarchy, the physics of the flow are best amenable to numerical prediction by scale-specific strategies.

Cross-scale interactions (forward and backward flow of information between the micro-, meso-, macro-scales) require merging of the solutions delivered by scale-specific approaches at each level of the scale hierarchy. Considering the top-down path, the computations at each level provide the boundary conditions needed at the lower levels. On the inverse path, starting from the bottom up, the computations at each level will deliver the closure laws needed at the higher level. For example, local, detailed CFD computations may deliver the heat transfer coefficient needed to describe the behaviour of a component, and component behaviour will provide the information needed at the system level. Examples of this cascade of computations are given in [16]. A "grand challenge" the CMFD treatment of Critical Heat Flux (CHF) will require such a cascade of computations [15]. The way to such multi-scale treatment requires of course mastering of the methods needed at each scale *and* producing the experimental data appropriate for their validation, again at each scale. In this paper we will review the extensive work related to bubbly flows, plumes and jets that has been conducted the last decade at PSI, guided by the perspective outlined above.

Needs for new kinds of experimental data

Until now, most of the two- or multi-phase computational work relied on closure laws derived from rather old fashioned experiments. Most of the data presently available and used for classical code validation work were obtained in essentially one-dimensional (1D) geometries and only average flow parameters (void fraction, heat flux, velocities, average temperatures or at most the time-average profiles of such variables, were measured. The validation of the CMFD methods requires new kinds of much more detailed and sophisticated experimental data such as three-dimensional flow field data.

An example of a recent project whose primary objective was to enhance the three-dimensional, two-phase flow prediction capabilities of current thermal-hydraulic codes for safety-relevant phenomena in present-day and future Light Water Reactors (LWRs) is ASTAR [17]. The new capabilities were to be validated by means of benchmark problems, and against data from a comprehensive set of new experiments in the bubbly flow regime. These 3D validation experiments have been performed using the LINX facility at PSI [18] and are discussed below.

PSI experiments with bubbly plumes and jets

A number of experiments were conducted over the last decade at PSI to study in detail the characteristics of bubbly plumes and jets and to provide the necessary experimental data needed for the verification of the CMFD models and codes used for their simulation. The motivation for this work came from the need to better understand Boiling Water Reactor (BWR) containment phenomena, in particular the behaviour of bubbly plumes in large liquid pools and the related mixing and stratification of the Pressure Suppression Pool (SP). Indeed, in a variety of conventional or "passive" BWRs, like the ESBWR, several scenarios lead to the injection of mixtures of steam and non-condensable gases from various types of vents into the SP. Injection from vents equipped with spargers will produce bubbly plumes. A second motivation for some of the early PSI work came from the scrubbing of aerosols - produced in case of a severe accident - in a pool. The first step in this direction was the study of the injection of gases from vents in pools and of the characteristics of the bubble plumes produced.

Bubbly plumes are also produced in a numerous industrial or natural situations, for example, the venting of steam and/or non-condensable gases into liquid pools in chemical reactors, gas stirring of liquid metal ladles, the aeration in water purification and waste treatment plants, the production of barriers against crude oil spread on water, blowouts of underwater gas lines, etc. Consequently, there

are a large number of experiments and publications for bubbly plumes in pools and to a lesser extent for bubbly jets. The interested reader will find literature searches in the three doctoral dissertations that produced most of the experimental work discussed here [19-21], as well as in the theoretical one [22] that accompanied the experiments. Most of the past experiments produced, at best, only *time average* profiles suitable for the verification of the existing classical global plume behaviour models [23]. Indeed these models are based on assumed profiles of the variables (typically Gaussian) and integral mass and momentum balances along the plume. A key element is the determination of the entrainment coefficient that specifies the amount of liquid entrained into the plume from the surrounding medium; this coefficient is obtained from the experimental data. Although the PSI experiments can be used of course for validating integral plume models, they also provide the much more detailed information needed for the validation of CMFD methods. Bubbly plume experiments *including* local measurements were carried out only in a few cases; for information regarding these tests, see Refs. [19-21,24].

Bubbly jets, in contrast to bubble plumes, have an initial momentum. The latest experiments with bubbly jets that, at some distance from the injector, lose their initial momentum and become essentially also buoyant bubbly plumes covered continuously the range between buoyant and forced plumes or jets. The early experiments with an upward facing single gas nozzle [19,24] provided the range of bubble sizes that are produced naturally from break-up of the initial gas jet in this case. The later experiments in the LINX facility were conducted with an injector carefully constructed to produce mono-disperse bubbles [18]. A special injector that could produce mono-disperse bubbles, "at will," in a range of diameters was created and used for the bubbly jet experiments [25]. All experiments were conducted in vessels having horizontal dimensions of the order of 1-2 m filled with demineralised water at atmospheric pressure. The bubble sizes were of the order of a few millimetres. The salient features of these experiments and the main findings will be discussed in the following sections.

The instrumentation used included double-tip optical sensors (DOS) for void fraction and bubble velocity measurements, hot-film anemometers (HFA) for liquid velocity measurements, photographic and video recording techniques, three-dimensional Electro-Magnetic Probes (EMP) for liquid velocity measurements, and PIV in the latest series of tests. The DOS and HFA techniques were extensively tested and the systems were calibrated and optimized during the early stages of the work [19,18]. The bubble velocities were determined with the DOS by measuring the time of flight of individual bubbles between the two consecutive tips (separated by a known distance).

The PIV equipment was capable of measuring both liquid and bubble velocities. It was commercial equipment with a dual YAG laser (532 nm, 100 mJ) and 1x1 kpixel cameras with one-byte gray level. This system is able to record and process in two-frame cross-correlation mode up to 15 couples of pictures per second. Glass filters fixed on the camera lens were used to select either the green laser light reflected by the bubbles or the orange light emitted by fluorescent seeding particles sprinkled in the flow and excited by the laser. This allowed *non-simultaneous* measurements of the velocity fields of both phases with a *single* camera and *simultaneous* ones with *two* cameras. The two-camera simultaneous-measurements technique clearly opened up new experimental avenues. The laser produced a 2-mm-thick vertical light sheet placed at the centre of the bubble injectors. The size of seeding particles was chosen as a compromise between visibility, which is related to the light emitted, and their capability to follow the flow. Details can be found in Refs. [20,26].

Latest experiments

The last two experiments conducted in a new test rig and a bubbly jet [21] and with *variable* but uniform bubble sizes and a bubbly plume in the LINX facility [18] with uniform bubble sizes. In this last phase of the work *simultaneous* measurements of the liquid and velocity fields were made possible by the addition of the second PIV camera. These experiments produced very large and unique data sets that should be very valuable for code validation.

Although the time-average behaviour of bubbly plumes has been studied fairly extensively in the past, the new data provide very interesting insights about the *instantaneous* plume behaviour. For example, the instantaneous *relative* velocities of the bubbles were measured and their average was confirmed to be different from the difference of the local averages of gas and liquid velocities, as expected but not confirmed earlier. Such information is needed for comparisons with time-dependent computations, for example, using Large Eddy Simulation (LES) techniques for bubbly flows modelled with the interpenetrating-media (two-fluid) formulation.

Although past work has focussed on the time-average behaviour of plumes and jets typically in two dimensions (either as two-dimensional sheets or axisymmetric round plumes), when examined closely, both exhibit strong three-dimensional characteristics as they meander and move in time and as instabilities develop in the shear layers. A unique feature of the recent experiments is that they were conducted in a manner that allows ensemble averaging of this kind of time-dependent data. The bubble plumes are naturally unstable and their meandering and oscillations create spreading of the average velocity and void fraction profiles well beyond what would have been observed in "stable" configurations. Indeed, examined on an instantaneous basis, the spreading is much less. It is evident that turbulence and other information extracted from the *time-averaged* fields is not representative of the instantaneous situation. Special techniques were used to overcome this difficulty, as discussed in more detail below. In this respect, the two sets of data provide unique and very interesting insights that await the interest of the CMFD analysts.

The companion question to the CFD or CMFD analyst is an interesting one. Bubbly flows have often been simulated with the two-fluid model. The forces acting on a single bubble were used as the basis for developing the interfacial interaction laws and the turbulence in the liquid was modelled with the RANS model. The results of such simulations were then confronted with time-averaged experimental data and the closure laws "verified" or adjusted accordingly. The intriguing fact is, however, that although the time-averaged experimental data and simulations may agree, the instantaneous physical picture is quite different. For example, the instantaneous spreading of the plume can be much less than the well-predicted average one. There may be no obvious answer to this problem within the framework of time-averaged RANS computations. The obvious way to tackle the problem is by simulating and comparing the *time-dependent* behaviour of the plume, something that seems to be an excellent candidate for Large Eddy Simulations (LES).

Experimental Work

Experiments with gas jets from single nozzles

As there were still few detailed systematic and complete studies of bubble plumes in relatively large pools, Kubash [19,24] conducted a new series of well instrumented and controlled experiments. The initial break-up of a jet created by injection of air through a single nozzle (diameters of 5, 10 and 20 mm) at the bottom of a pool filled with water was of particular interest. The pool was 1 m in diameter and pool depths of up to 3 m were investigated. The gas injection velocities varied between

1.2 and 152 m/s at the exit of the nozzles. The air flow rate was limited to minimize oscillation of the entire plume in the pool. Demineralised water was pumped into the tank at the bottom at a very low velocity (2.1 mm/s) and collected by an overflow section at the top.

The plumes had two distinct regions: a zone of flow establishment (ZFE) close to the nozzle and a zone of established flow (ZEF) further downstream. The bubble plume in the ZEF was buoyancy driven as the initial jet momentum has dissipated and bubble break-up was rather complete; the initial jet conditions did not affect significantly the plume characteristics in the ZEF. This important finding was made with systematic investigations at constant air flow rate but with different nozzle diameters.

Void fraction, bubble and water velocity profiles collected at different elevations provided information about the expansion of the bubble plume in the horizontal direction. Figure 1 shows typical void fraction profiles. The profiles were fitted with Gaussian curves

$$\varepsilon(r,z) = \varepsilon_m(z)\exp\left(-\frac{\left(r - r_{c,\varepsilon}(z)\right)^2}{b_\varepsilon^2(z)}\right),$$

where ε is the void fraction, r the radial distance and z the vertical coordinate. The plume width b_ε describes and correlates the horizontal expansion of the bubble plume; it was found to increase linearly with z, confirming previous results. Similar fits and linear correlations were produced for the liquid velocity.

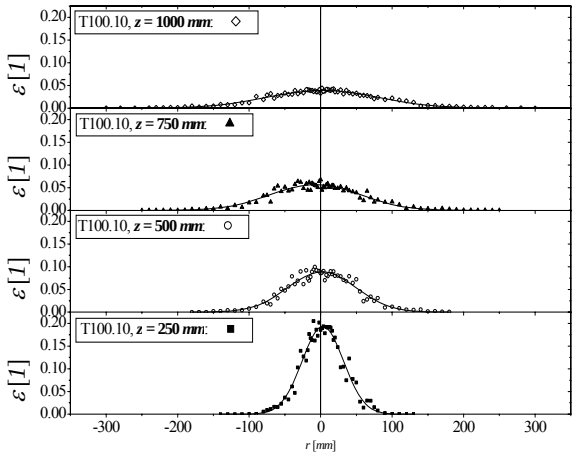

Fig. 1 Radial void fraction profiles at four distances from the nozzle, in the zone of established flow (air flow rate, Q_{air}= *100 l*$_n$*/min,* nozzle diameter d_{nozzle}= *10 mm*).

Comparison of the void-fraction and liquid-velocity profile's spreading rates shows a bubble core within an entrained water flow area that expands radially beyond the bubble core. The fact that the liquid plume expands more widely than the bubble core can be described with the ratio between b_ε and b_w, the corresponding liquid velocity width. The data in the present tests have shown that this value is about 0.8 for all tests and at each distance from the nozzle, a very useful and universal result.

The bubbles rise in the entrained water flow, and so their velocity in the plume is considerably higher than that of individual bubbles in stagnant water. Bubble chord length distributions were fitted with log-normal distributions and provide information on the bubble size spectrum.

A semi-empirical bubble plume model, used previously in relation to lake venting phenomena, could be used to describe the global characteristics of the flow using model parameters derived from the older experimental data, where, however, the void fraction was about ten times lower than in the present tests. Good agreement was found between the experiments and model predictions, indicating that such models are applicable to the flow conditions in the present work.

Bubbly plumes in LINX

Basic time-average measurements

Bubbly plumes were investigated within the framework of the ASTAR project [17], as mentioned in the introduction [18]. These experiments were conducted in the LINX facility, Fig. 2, a well instrumented and controlled cylindrical vessel, 2 m in diameter and 3.4 m in height. The facility is equipped with twelve glass windows located on the sides to permit observations from outside.

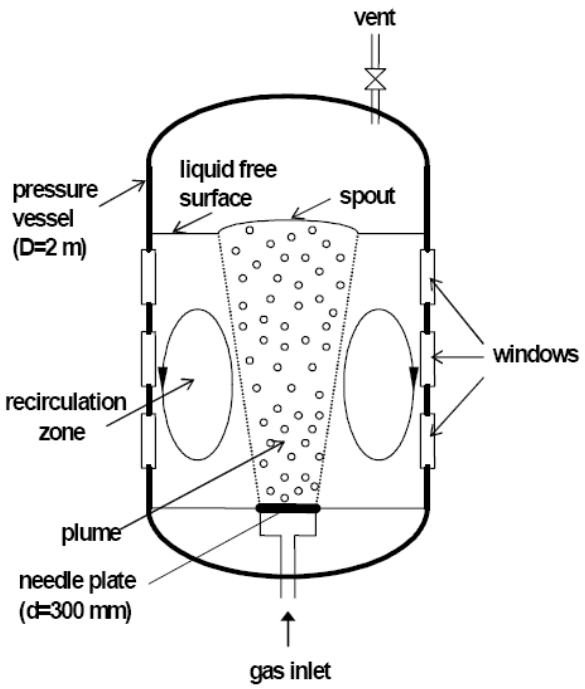

Fig. 2: Schematic of the plume experiments in the LINX facility.

An air injector was installed near the bottom of the LINX vessel that was partly filled with water to a depth of 1.5-2 m. This injector was quite different from that of the previous experiments by Kubasch. It was a multi-needle injector, specially designed to create a large, axisymmetric bubble plume with bubbles of uniform size. The gas flow rate to the injector was kept relatively low in order to ensure that there is practically no coalescence or break-up of the bubbles. Around the plume, a large-scale recirculation flow was generated, as shown schematically in Fig. 2.

The injector consisted of 716 small tubes of 80 mm height and 2 mm inner diameter, distributed uniformly over a circular area of 0.3 m in diameter near the bottom of the vessel. Each injector tube was fed via a smaller-diameter, 0.8 m long and 0.3 mm inner diameter capillary from a common gas supply header. This arrangement of a large number of parallel, highly-throttled injector tubes assures stable, uniform flow rates for all the needles and consequently uniform bubble generation. The injector produces a broad, axisymmetric bubble plume with bubble diameters around 3 to 4 mm. The geometrical arrangement of the needles ensures that there are no interactions between neighbouring bubbles close to the injection region.

Void fraction, bubble mean diameter and velocity have been measured at various elevations using double-tip optical probes. PIV has also been implemented in order to investigate the liquid and bubble velocity fields in a vertical plane passing through the centre of the injector. The measurements for the liquid and the gas fields were produced in sequence with a single PIV camera. In addition to these instruments, a multi-electrode electromagnetic current meter (EMP) has been utilized for determining the liquid velocity pattern in the recirculation zone [18,26,27].

Figure 3 shows the measured radial void-fraction distributions in the plume with the DOS at several gas injection flow rates. At low elevations, close to the injector (Fig. 3a), the void fraction exhibits a top-hat-like distribution: roughly flat above the 0.3 m diameter injector, dropping rapidly at the edges. At higher elevations (Fig. 3b), the distributions are more spread out, with the centre-line value decreasing as the plume spreads and its profile becomes Gaussian.

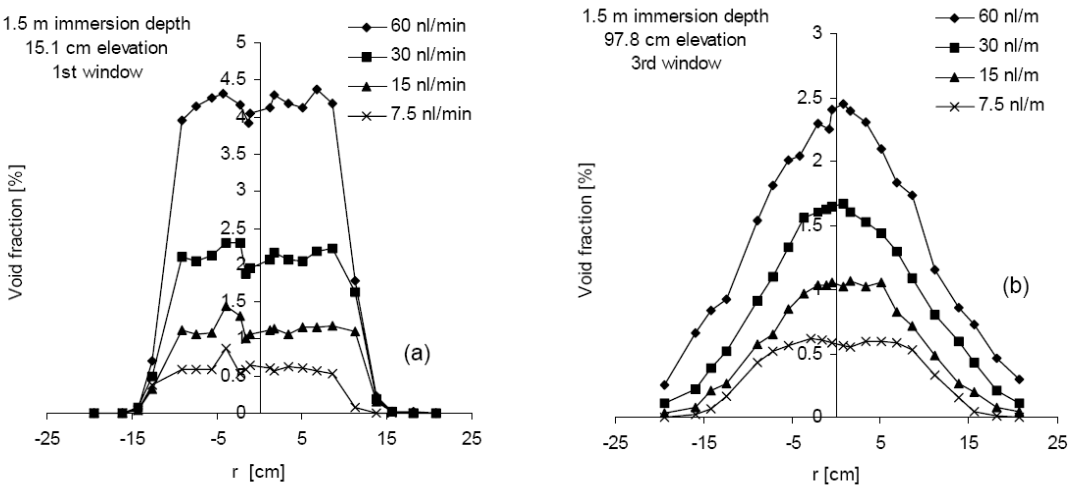

Fig. 3. Void-fraction distributions for different injection flow rates: (a) close to the injector, and (b) far from the injector. Both figures correspond to a 1.5 m immersion depth.

The vertical component of the bubble velocities from PIV and from DOS were compared and showed reasonably good agreement, although the optical probes give slightly higher velocities. The reasons are discussed in [27].

In spite of the fact that the plumes exhibited unsteady (fluctuating) behaviour, the distributions of the long-time average values of the different plume variables were found to be axisymmetric. However, the fluctuations led to a broadening of the time-averaged profiles; this matter was fully investigated and quantified in the experiments that followed.

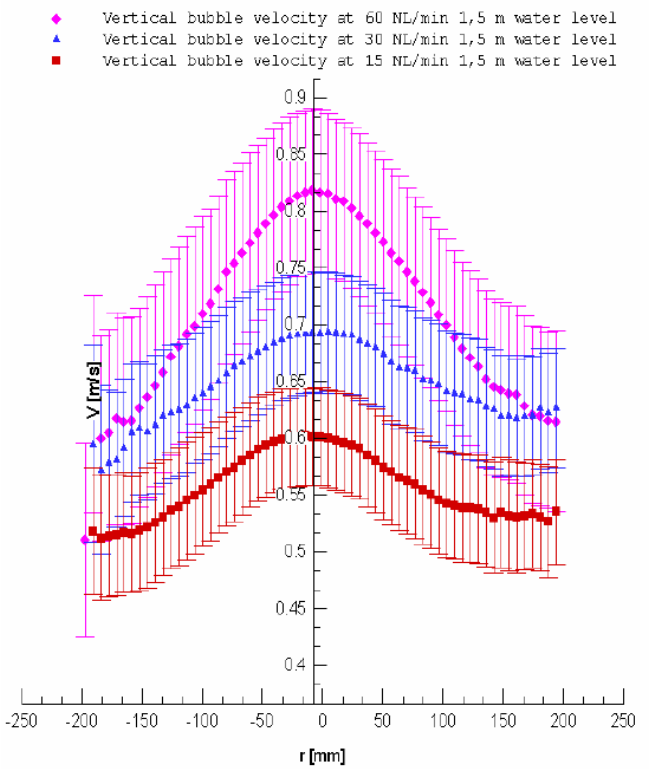

Fig. 4. Radial profiles of the vertical bubble velocity obtained by PIV for several injection rates.

Figures 4 and 5 show the gas and liquid velocity distributions at several gas flow rates. The details of the experiments can be found in Refs [18,20].

Typical apparent centreline position and apparent plume diameter pdfs are shown in Fig. 6. The word "apparent" is used here as a reminder of the fact that the plume centreline is most of the time not on the PIV plane and what is observed is indeed a "chordal" cut of the plume. Figure 6a shows a clear increase of the scatter of the instantaneous position of the plume centreline between elevations 250 mm and 600 mm, but no significant further spread above 600 mm.

In Fig. 6b, the pdf of the apparent plume diameter, D_{App}, is plotted for three elevations. Due to the meandering, the measured apparent diameter, actually a chord as already mentioned, is always smaller than the real diameter. An estimation of the maximum error due to the out-the-PIV-plane displacement of the plume axis was made [28] assuming that the instantaneous horizontal cross-section of the bubble plume is circular and that the distribution of the out-of-plane displacement of the centreline position is the one given in Fig. 6a. Therefore, for each D_{App} in Fig. 6b, the real diameter D will have a

value between D_{App}, in case of nil out-of-plane displacement, and the values $D = f(Delta_{max})$ given in the figure. $Delta_{max}$ is the radius of the circle where the centreline of the plume was confined for the particular ensemble average.

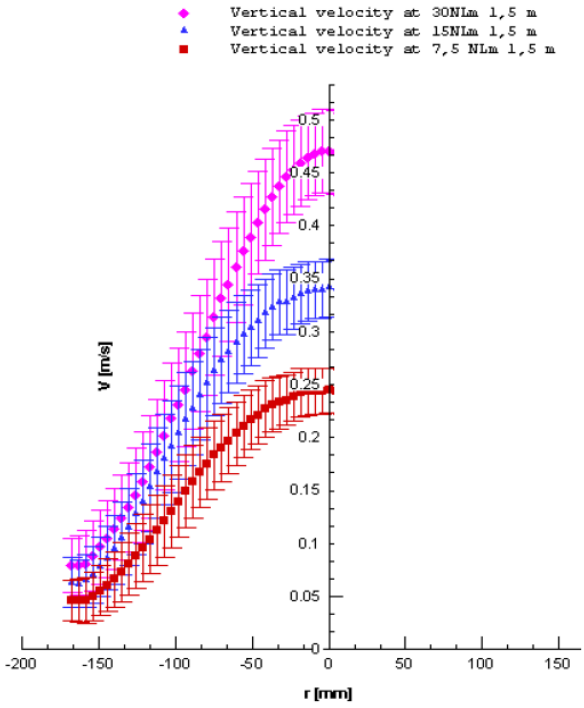

Fig. 5. Influence of the gas injection rate on the vertical liquid velocity distribution. Only half of the bubble plume could be measured reliably due to the attenuation of the laser light by the bubbles.

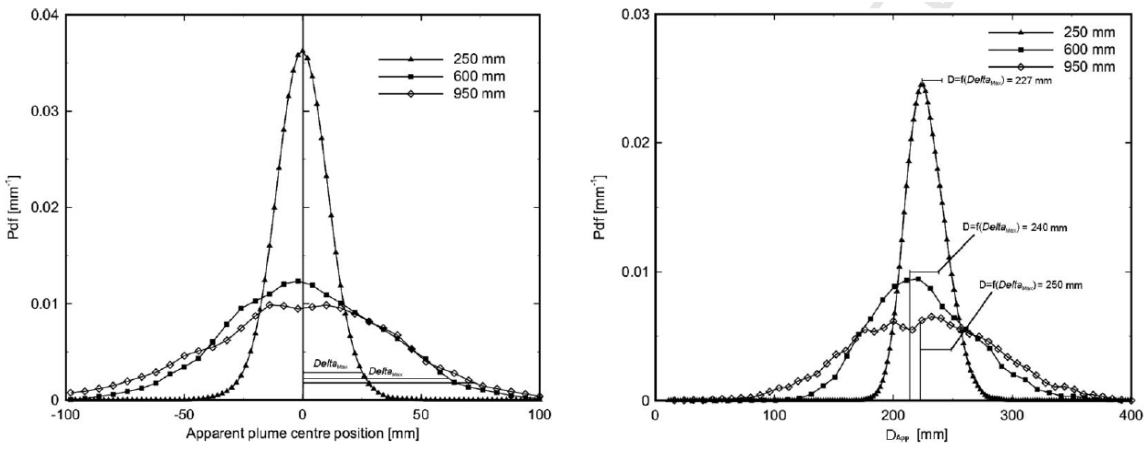

Fig. 6. Experimentally measured distributions of the apparent plume centerline position (a), and of the apparent plume diameter (b) at three elevations, at 30 Nliter/min.

The apparent diameter distribution at 250 mm above the injector, Fig. 6b, shows a most probable value at 220 mm, which would lead to a real diameter in the range 220 mm < D < 224 mm for a

Delta$_{max}$ of about 20 mm. These *D* values are smaller than the injector diameter of 300 mm. Indeed, visual observations of the plume revealed that a strong contraction occurs just above the injector. At higher elevations, 600 and 950 mm in Fig. 6b, the pdfs became broader and larger. The *means* of these pdfs, estimated with the correction mentioned above show plume diameters *D* in the ranges of about 210–312 mm and 220–250 mm, with *Delta*$_{max}$ of about 60 and 65 mm, respectively. The wider distributions at higher elevation are due to the larger plume width oscillation and to the 3D plume structure motion which appear as a fluctuation of the apparent plume diameter. At about two-thirds of the total plume height, the 950 mm elevation in Fig. 6b, the pdf of the apparent plume diameter shows also a saturation effect similar to that of the centreline plume position. These results are contrary to the classical ones that state that the *average* plume width continues growing. Additional evidence is apparent in Fig. 7, where the time-average bubble velocity field shows axial spreading, while an instantaneous shot none.

The database assembled from these experiments forms a valuable, consistent set, and can therefore be used for the validation and development of advanced, numerical, two-phase flow simulations. Limited data from the database will be released as part of PSI's commitment to the NURESIM project. Mainly instantaneous experimental data will be used e.g. for validating the modelling of turbulent stresses, for comparison with LES predictions (3D and time-dependent), to help understanding instantaneous plume behaviour (flow pattern development), etc.

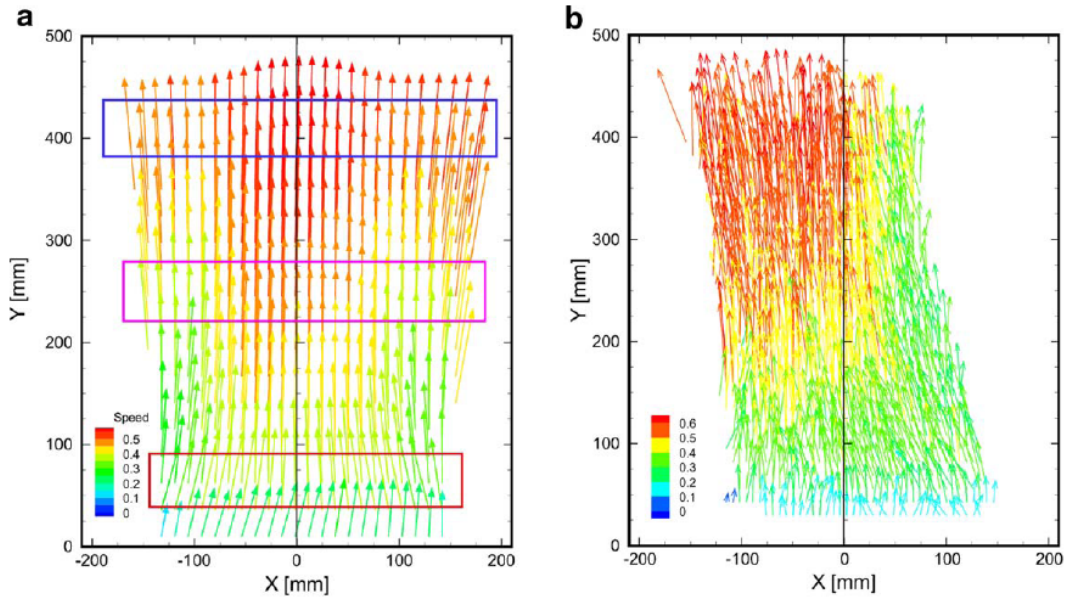

Fig. 7. Time-averaged (a) and instantaneous (b) velocity fields. Injection rate of 30 Nliter/min.

Time-dependent, simultaneous two-phase measurements

The earlier experiments in LINX showed that the plume was meandering and that time averages of the profiles were "artificially" spreading the plume, while its actual spread observed at any *instant* was much less, as expected in fact. Instantaneous measurements of plume parameters cannot be conducted and single measurements are not very useful; the DOS require long time averaging to yield meaningful results; even PIV, 2D flow fields are too noisy and also need time averaging to yield useful quantities. As all time-average measurements, and in particular measurements of the fluctuating quantities are necessarily affected by the large-scale motions of the plume, a way to deal with this

problem became necessary. The first thought was to "stabilize" the plume in the vessel, but it became evident that this would have led also to unwanted distortions and it would have been an unnatural situation. Then came the idea to "profit" from the time-dependent 3D nature of the plume and collect the data in a novel way that could yield interesting results; this approach is outlined now.

PIV was used again in the latest series of LINX experiments to *simultaneously* measure the instantaneous phase velocities and the relative velocity in a vertical plane crossing the injector (using *two* PIV cameras now). However, now, in addition, an independent, two-camera video recording system stored images of the bubble plume structure from two perpendicular directions, allowing categorization of the PIV data according to the instantaneous state of the plume. Thus, the instantaneous bubble, liquid and relative velocity vector plots obtained could now be correlated with the corresponding instantaneous plume state obtained from the video recordings. The video images were treated to produce parameters, such as the plume projected diameters (or rather axes) and plume centreline position that were then used to characterize and select the subsets of data for the ensemble averages. The procedure is clearly not simple; success during the first series of tests conducted this way is, however, very encouraging.

As the plume meanders in the vessel, its instantaneous shape (for example, characterized by its projected average diameter in a 2D window view) changes; the plume "centre" (not forgetting the fact that the instantaneous plume cross section is not really circular) moves in and out of the PIV plane; The plume "centre" has also a certain direction of motion and velocity. Considering all these effects, true ensemble averages according to the state of the plume would have required sampling of the flow field images according to all the parameters enumerated above, something that would have required a huge data set and a data mining and reduction effort that was beyond the scope of the first experiments. A more modest ensemble averaging – limited to cases where the plume centre was on the PIV plane and its apparent diameter had a certain range – validated the method and already produced very interesting results, in particular in relation to the fluctuating quantities. The existing extensive data sets can, however, further be mined to yield additional insights and information.

First ensemble-average results [30] are briefly discussed below. Although ensemble averaging has been discussed often in the past as *the* method for tackling fluctuating two-phase flows, such data have never been produced before in a situation similar to that of a bubble plume, to the authors' best knowledge. The new technique is not simple, but opens broad new perspectives, in particular in relation to its use in conjunction with novel analytical techniques such as LES applied to two-phase flows, as already mentioned in the introduction.

The relative velocity, estimated as the average of the instantaneous local phase velocity differences rather than the difference of the two phase velocity averages, showed unexpected axial and radial evolution [29].The authors suggest that, due to their helicoidal-zigzag motion through the variable-liquid-velocity region, the bubbles never reach their terminal velocity.

In addition to the above measurements of the classical plume variables, several turbulent quantities were also measured, including the spatial distributions of the time-averaged stress tensor, turbulent intensity and turbulent kinetic energy. The turbulence was highly anisotropic, as expected and the origin of the turbulent production terms was identified according to the presence in the plume of different phenomena (meandering, pulsations, shear, plume contraction, etc.). Details can be found in Ref. [29].

Some of the latest, most interesting results where ensemble averages of *fluctuating* data were also produced are presented next [30]. Near the injector, the plume was rather stable, while higher up it exhibited the meandering and oscillations discussed earlier. Taking advantage of this fact,

measurements of the stress terms were produced at both ranges of elevations; simple time averages were produced at the lower elevations, while ways for separating the effects of the large-scale motion due to meandering from the small-scale effects of turbulence had to be found for the higher elevations. A few indicative results are given below. The details of the work [20] will be presented in papers in preparation [29,30].

Stress terms at lower elevations

Several turbulent quantities were measured, including the spatial distributions of the time-averaged stress tensor, turbulent intensity and turbulent kinetic energy. Turbulence is shown to be highly anisotropic with strong shear-induced generation mechanisms which were measured separately [20,29].

Figure 8 shows the normal and the shear stresses for the liquid phase (subscript L), $\overline{\tilde{u}_L'\tilde{u}_L'}, \overline{\tilde{v}_L'\tilde{v}_L'}, \overline{\tilde{u}_L'\tilde{v}_L'}$, obtained at the gas flow rate of 15 Nliter/min, at different elevations, starting with the one closest to the injector, at about 266 mm, and moving further up to the 438 mm elevation. (The tildes are to remind the reader that some space and time filtering processes took already place by the PIV process itself.) An interesting evolution of peak values can be observed in all the stress terms, presenting a clear correlation with the average liquid velocity gradients observed. The stress distributions show two peaks marked as 1, 2 at the two lowest elevations, at about r = 65 mm from the injector centreline. These peaks correspond to the sharp edge of the liquid velocity profiles measured at the same elevations. At higher elevations (285 − 312 mm elevations), the peaks marked as 3, 4, 5, shift to shorter radial distances, with smaller or comparable stress values in accordance with the liquid velocity slopes observed at these locations. Moving away from the injector (372−438 mm elevations), the peaks 6, 7, 8 move towards the centre at about r =45 mm and show a significant jump in intensity. This shift is again another manifestation of the observed bubble plume contraction. Comparing the radial and downstream directions Figure 8 clearly confirms that turbulence is strongly anisotropic.

Time-dependent measurements with ensemble averaging at higher elevations

As noted above, at the higher elevations where plume meandering was very strong, ensemble averages were produced in order to separate the effects of the meandering from those of the turbulence inherent to the plume. A triple decomposition was assumed for the measured variables:

$$\tilde{\phi} = \bar{\tilde{\phi}} + \tilde{\phi}_{meand} + \tilde{\phi}',$$

where the effects of large-scale meandering (subscript *meand*) and small-scale turbulence (primed quantities) are separated. One can estimate the effect of meandering by comparing data averaged at a point "globally," i.e., by ignoring the effect of meandering and data that are ensemble averaged according to the selection criteria discussed above. An early example is shown in Fig. 9, where both the velocity profiles and the Reynolds stress term are plotted. In this case the ensemble averaging was simply restricted to the minimum, considering only the PIV data for which the plume centreline was within a radius of 5 mm from the injector centreline in the PIV observation window (*Delta* = 5 mm). The expected effect of the ensemble averaging on the vertical liquid velocity profile is obvious; the globally averaged profiles are flatter, as expected. The Reynolds stress term shows a clear reduction with ensemble averaging. The difference can be attributed to the effect of the meandering (not forgetting the imperfections of this first ensemble averaging, also noted above; more sophisticated treatment of the data is underway [30].

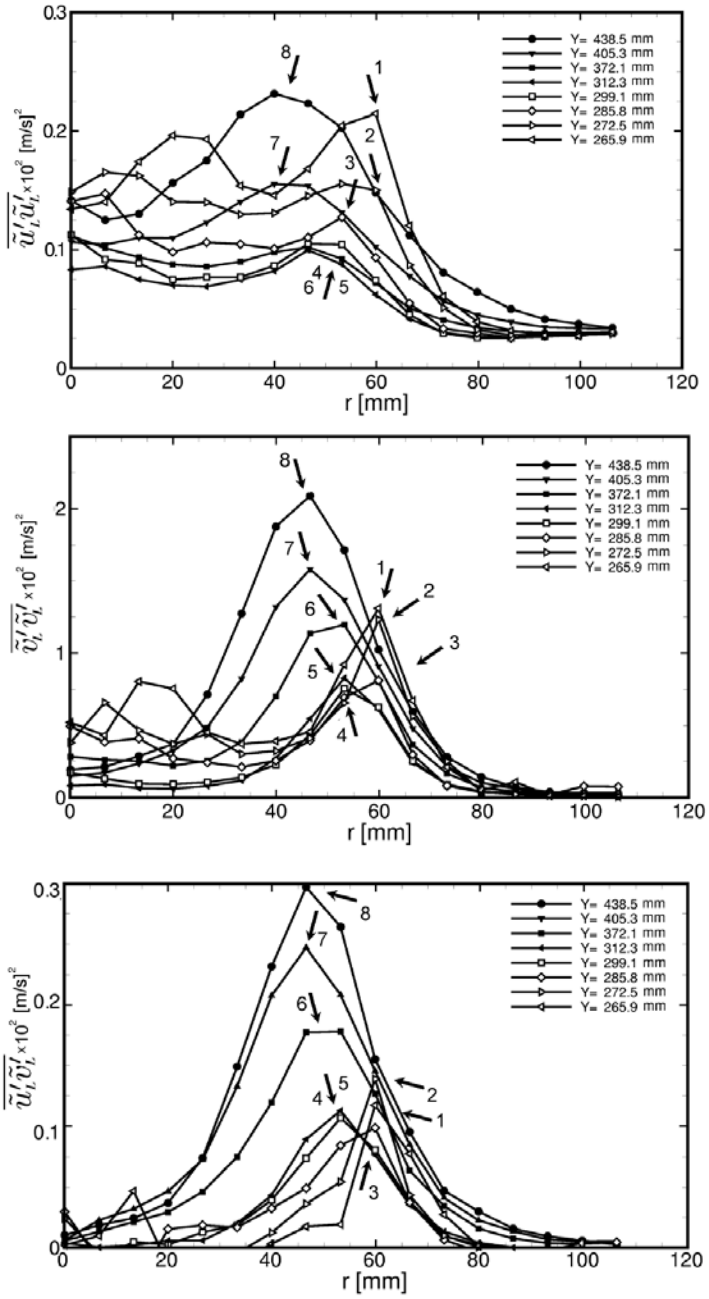

Fig. 8. Stress term profiles of the liquid phase at the injection rate of 15 NLiter/min at various elevations. At the lower elevations of the figure plume oscillations and meandering were minimal.

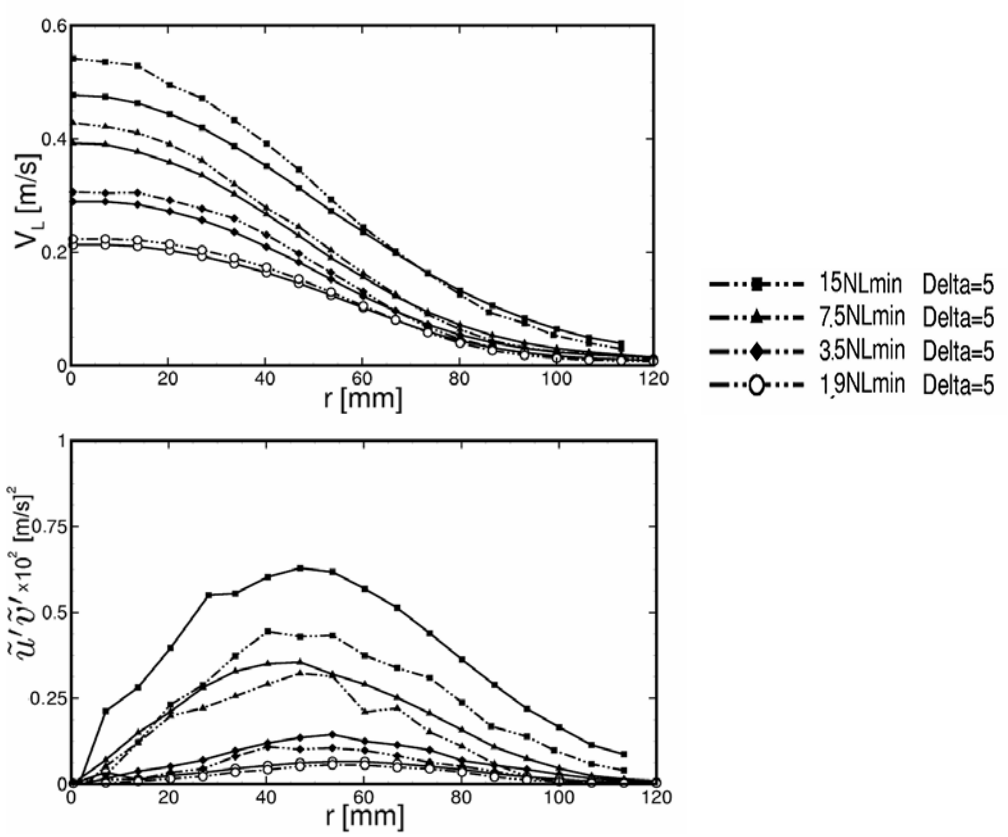

Fig. 9. Global averages (solid lines) and ensemble averages (dotted lines) at various elevations away from the injector. Liquid velocity profiles (left) and Reynolds stress term (right).

Bubbly jet experiments

The second set of recent experiments discussed here [21,31,32] was carried out with bubbly jet flows generated by a specially designed gas/liquid injector. One aim of these experiments was to study the interactions between coherent structures and bubbles, as well as the feedbacks from bubble agglomeration on the development of these structures.

The bubbly-jet injector and a schematic of the experiment are schematically shown in Fig. 10a. The patented injector has been developed after a series of experiments carried out to determine the optimal configuration of tubes and needles for forming bubbles with uniform size in the range between 1 and 6 mm [25]. The bubbles are formed by continuously injecting air (AF) through the needles into the co-currently flowing internal water flow – IWF. The jet flow is formed afterwards by adding the second, external water flow – EWF.

The shear layers in the jets become unstable and generate large coherent structures or vortices, as sketched in Fig. 10a. The interactions of the coherent structures with the bubbles produce a mine of experimental information about the interactions of bubbles with the surrounding liquid and liquid turbulence. Naturally-developing instabilities and structures in the shear layer are impossible to study because of their instantaneous and to some extent random nature (like the natural meandering and the oscillations of the bubble plumes). Periodic triggering of the jet at frequencies in the neighbourhood of

the naturally developing ones produces much more reproducible structures. The excitation was achieved by periodically modulating the jet shear layer by means of a coaxial water layer injected close to the jet exit through a separate annular nozzle, Fig. 10a. The triggered structures have been studied by ensemble averaging, in this particular case, phase-averaging, since the period of the excitation was well defined. The signals from the instruments (PIV and DOS) were collected only at certain phases of the triggering period. By varying this phase systematically the entire excitation period can be covered. Milenkovic and co-workers [21,25,31,32] perfected this *vortex tracking* technique that yielded very interesting and unique results. A few typical results will be shown below.

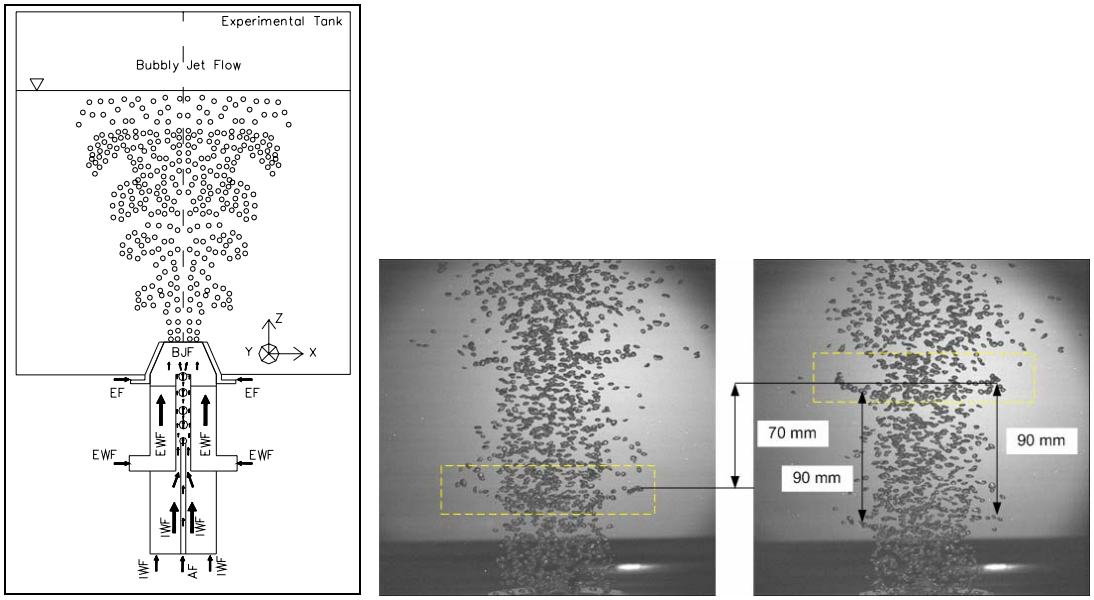

Fig. 10. Schematic of the bubbly jet experiment showing at much larger scale the principle of the injector (left, a). Instantaneous images of the bubble ring at two different phases of the excitation period with 267 ms delay (right, b).

Special emphasis had to be attributed to the synchronization of the experimental PIV measurements, the photographic recordings and the DOS measurements with the external triggering of the flow structures. Another unique aspect of the experiment was the use of mono-disperse and controlled-diameter bubbles. In addition to DOS and PIV, other experimental techniques like, Laser Induced Fluorescence (LIF) and shadowgraphy were also used.

In Milenkovic's work [21,31,32] both jet flows with constant inlet flow rates of liquid and gas (the "naturally-developing jets") and periodically excited jets with controllable frequency and amplitude, or "triggered jets," were investigated. When bubbles enter the vortex rings that develop in the shear layer, they can be trapped if certain conditions are fulfilled. Milenkovic [21,31,32] has developed a bubble trapping criterion based on the forces acting on the bubbles and successfully confronted its predictions to the experimental results. This kind of investigation can lead to valuable insights about the adequacy of the bubble-liquid interaction laws used.

To quantify the interaction between bubbles and the large vortices that are formed in the shear layer, the following phase-averaged quantities were determined by two-phase (liquid and gas) PIV: the azimuthal liquid vorticity field, and the vertical velocity of liquid and bubbles. The vertical velocities of both the vortex rings that are formed and those of the bubble rings that develop from trapped

bubbles, Fig. 10b, were also estimated. The data were acquired at different phases within the triggering periods. The azimuthal liquid-vorticity field provides interesting information on intensity, size, shape and position of large vortices in the flow field, Fig. 11.

Phase-averaged DOS data were also collected revealing the periodic variation of the void fraction in the shear layer and providing information on the clustering of the bubbles in coherent vortex structures, with a periodic variation of void fraction during the excitation period, Fig. 12. Again, these experiments produced a huge amount of data that has only been partially analyzed and exploited so far.

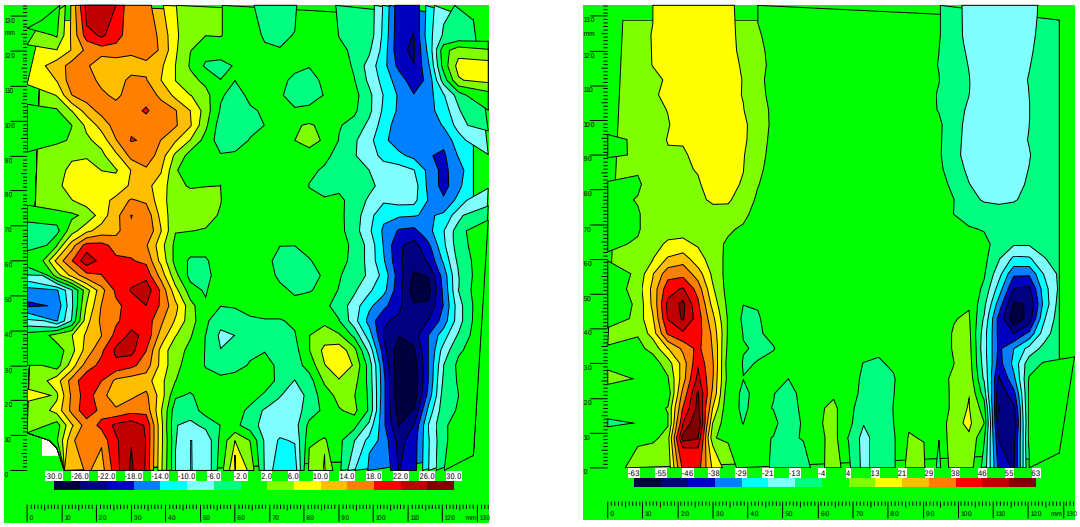

Fig. 11. Iso-vorticity contours of a bubbly jet. Left: naturally developing jet. Right: triggered jet at a certain phase of the excitation period.

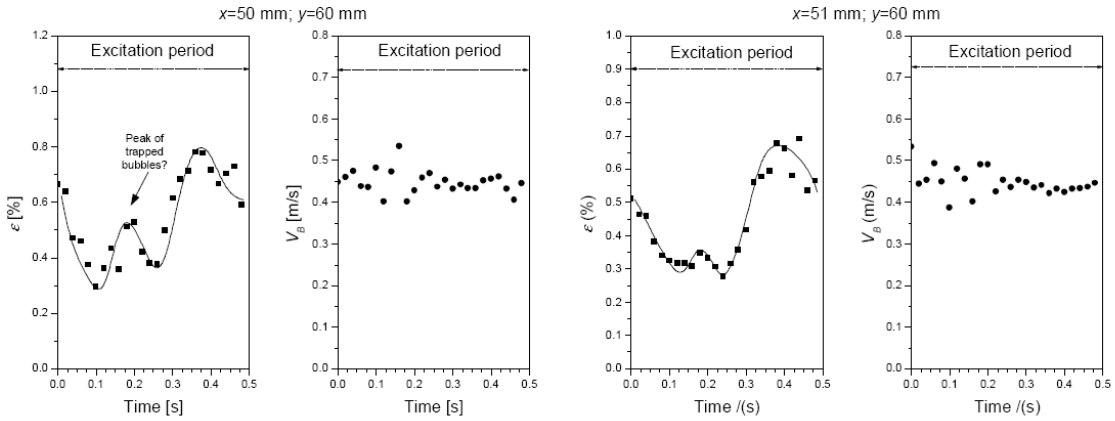

Fig. 12. Variation of the phase-averaged void fraction and of the vertical bubble velocity measured by DOS during an excitation period at the vertical position y = 60mm and points in the shear layer at x = 50 and 51mm.

Analytical developments

Dealing with turbulence

The classical methods for dealing with turbulence, i.e., the Reynolds-averaged Navier-Stokes formulations (RANS), are being complemented now by more advanced formulations such as Large Eddy Simulation (LES), which are much more appropriate for dealing with certain flow situations: they seem to be particularly useful in relation to certain classes of two-phase flows, such as bubbly flows [22].

Bubbly flows – for which turbulence in the transporting phase, partly generated by bubble motion, plays a determining role – have already been treated using CMFD. They have so far been tackled mainly by use of the two-fluid, interpenetrating-media model, in conjunction with the conventional RANS approach for turbulence. In this case, both turbulence and the interfacial exchanges are modelled. The use of Large Eddy Simulation (LES) to capture the turbulent interactions between bubbles and the energy-containing large eddies in the continuous phase seems a very promising line of approach, since it captures well the large eddies mainly responsible for the interactions with the bubbles. Interesting questions arise regarding, for example, the various flow scales: the scale of turbulence, the dimension of the bubbles and the scale of the LES cut-off filter.

These questions were addressed in a systematic study undertaken by Milelli and co-workers [33,34,35]. The major conclusions drawn from sensitivity studies made for corresponding flow configurations are as follows.

- The optimum ratio of the cut-off filter width (i.e. the grid) to the bubble diameter should be specified at around 1.5. Larger values than this lead to the transfer of a large portion of the energy-containing scales into sub-grid-scale (SGS) motions.
- The value to be assigned to the lift coefficient C_L was found to play a major role in plume spreading, with best comparisons obtained using C_L = 0.25. The authors also noted that 2D and 3D time-averaged quantities were almost identical, and compare very well with measured data (i.e. phase velocities and void fraction profiles).
- Finally, the turbulent energy spectrum taken in the bubbly-flow region revealed a power-law distribution which oscillated between -5/3 and -8/3 in the inertial sub-range, providing evidence that there was little impact of the dispersed phase on the liquid turbulence. The results conform to previous studies, which attributed the more dissipative spectrum to the presence of the dispersed phase.

LES of multiphase flow has now been extended to interfacial, sheared, two-phase flow in combination with interface tracking techniques [36, 37]. Liovic and Lakehal [36] incorporated the VOF approach, and applied it to the case of air/steam injection into a water pool, as investigated previously by Meier [38]. It is obvious that the available computational resources will not allow this approach to be used to capture the details of a dispersed bubbly flow, as is now dome routinely using the two-fluid formulation, but it does show promise that flows involving large interfacial inclusions may be tackled in the near future. Novel analytical developments to the method have now been developed [37], namely in the treatment of turbulence near sheared deformable interfaces. A combination of the Large Eddy Simulation (LES) and Interface Tracking (IT) procedures will probably represent the next challenge dispersed/interfacial two-phase flows.

Acknowledgments

The work reviewed here covers nearly a decade of experimentation and analysis at PSI and at ETHZ. The authors are indebted to several of their PSI and ETHZ colleagues for valuable contributions, discussions, advice etc.: M. Andreani, J. Dreier, J. Kubasch, M. Fehlmann, S. Güntay. The LINX experiments have been carried out within the ASTAR project of the 5th Euratom Framework Programme Nuclear Fission, with financial support from the Swiss Federal Office for Education and Science under contract No. 99.0796. The authors also gratefully acknowledge support from the Emil Berthele Fonds (ETHZ). The bubbly jet experiments were conducted with financial support from the Swiss National Science Foundation under contract Nos. 200020-103630, 21-61698.

References

[1] G. Yadigaroglu, Letter to the Editor, "CMFD (a Brand Name) and Other Acronyms," *Int. J. Multiphase Flow,* **29** (2003) 719–720.

[2] M. Andreani, F. de Cachard, K. Haller, M. Simiano, B.L. Smith and R. Zboray, "Basic Validation of CFD Codes for Containment Thermal-Hydraulics," *Proc. Annual Meting on Nuclear Technology,* Nürenberg, Germany, 10-12, May, 2005.

[3] M. Scheuerer, M. Heitsch, F. Menter, Y. Egorov, I. Toth, D. Bestion, S. Pigny, H. Paillere, A. Martin, M. Boucker *et al.,* "Evaluation of Computational Fluid Dynamic Methods for Reactor Safety Analysis (ECORA)," *Nucl. Eng. and Design,* **235** (2005) 359-368.

[4] O. Auban, R. Zboray and D. Paladino, "Investigation of Large-Scale Gas Mixing and Stratification Phenomena Related to LWR Containment Studies in the PANDA facility," to appear in *Nucl. Eng. and Design,* (2006).

[5] R. Zboray, D. Paladino and O. Auban, "Experiments on Gas Mixing and Stratification Driven by Jets and Plumes in Large-Scale, Multi-Compartment Geometries," *Proc. 14th International Conference on Nuclear Engineering (ICONE-14),* Miami, Florida, USA, July 17-20, 2006.

[6] D. Paladino, O. Auban and R. Zboray, "Large Scale Gas Mixing and Stratification Triggered by a Buoyant Plume with and without Occurrence of Condensation" *Proc. International Congress on Advances in Nuclear Power Plants (ICAPP 06)*, Reno, Nevada, USA, June 4-8, 2006.

[7] Paul Scherrer Institute and Commissariat à l'Energie Atomique, Saclay, "Proposal for the OECD SETH II Project to Resolve Key Computational Issues in the Simulation of LWR Containment Thermal-hydraulics," Proposal submitted to OECD/NEA.

[8] G. Yadigaroglu, "Computational Fluid Dynamics for Nuclear Applications: from CFD to Multi-Scale CMFD," plenary introductory lecture, pp. 51-58 in *FISA 2003, EU Research in Reactor Safety, Proceedings,* Luxembourg, 10-13 November 2003, European Commission EUR 21026. Also: *Nucl. Eng. and Design,* **235** (2005) 153-164.

[9] G. Yadigaroglu and D. Lakehal, "New Challenges in Computational Thermal Hydraulics," invited plenary lecture, *Proc. 10th International Topical Meeting on Nuclear Reactor Thermal Hydraulics (NURETH-10)* Seoul, Korea, October 5-9, 2003. Also: *Nuclear Technology*, **152** (2005) pp. 239-251.

[10] D. Lakehal, "DNS and LES of Turbulent Multifluid Flows," *Proc. 3rd Int. Symp. Two-Phase Flow Modelling and Experimentation,* Keynote Lecture, Pisa, Italy, Sep. 22-24, 2004.

[11] D. Bestion, H. Anglart, B.L. Smith, M. Scheuerer, M. Andreani, J. Mahaffy, F. Kasahara, E. Komen, P. Mühlbauer and T. Morri, "Extension of CFD Codes to Two-Phase Flow Safety Problems," Technical Note, OECD NEA/SEN/SIN/AMA(2006)2, July 2006.

[12] D. Bestion, “On the Application of Two-Phase CFD to Nuclear Reactor Thermalhydraulics,” *Proc. 11th International Topical Meeting on Nuclear Reactor Thermal Hydraulics (NURETH-11),* Avignon, France, October 2-6, 2005.

[13] G. Yadigaroglu, D. Lakehal, B.L. Smith and M. Andreani, “New Trends and Introduction of Multiphase CFD Methods in Nuclear Engineering,” *The International Conference on Multiphase Systems, ICMS'2000*, Ufa, Russia, June 15-17, 2000.

[14] G. Yadigaroglu, M. Andreani, J. Dreier, and P. Coddington, "Trends and Needs in Experimentation and Numerical Simulation for LWR Safety," *Nuclear Engineering and Design*, **221** (2003) pp. 205-223.

[15] D. Cacuci, “NURESIM: A European Platform for Nuclear Reactor Simulation,” *FISA: Conference on EU Research and Training in Reactor Systems,* Luxembourg, (2006).

[16] G. Yadigaroglu, "Application of Cascades of CFD Methods to Two-Phase Flow Problems,” *Trans. Inst. of Fluid-Flow Machinery* (Poland), **112** (2003) 47-55.

[17] F. de Cachard, H. Deconinck , G. Franchello, U. Graf, A. Kumbaro, S. Mimouni, H. Paillere, E. Romenski, P. Romstedt, J.M. Rovarche, B. Smith, H. Städtke, E.F. Toro and B. Worth, “The ASTAR Project - Status and Perspective,” *Proc. 10th International Topical Meeting on Nuclear Reactor Thermal Hydraulics (NURETH-10),* Seoul, Korea, October 5-9, 2003.

[18] R. Zboray, M. Simiano and F. de Cachard, “Confined Bubble Plumes: Description of the Facility and Experimental Results,” Paul Scherrer Institut Technical report, TM-42-03-22, (2003).

[19] J. Kubasch, “Bubble Hydrodynamics in Large Pools,” Doctoral dissertation, Swiss Federal Institute of Technology, ETH Diss. No. 14398, Zurich, Switzerland (2001).

[20] M. Simiano, “Experimental Investigation of Large-Scale Three Dimensional Bubble Plume Dynamics,” Doctoral dissertation, Swiss Federal Institute of Technology, ETH Diss. No. 16220, Zurich, Switzerland (2005).

[21] R. Milenkovic, “Experimental Investigation of Bubbly Jets,” Doctoral dissertation, Swiss Federal Institute of Technology, ETH Diss. No. 16206, Zurich, Switzerland (2005).

[22] M. Milelli, “A Numerical Analysis of Confined Turbulent Bubbly Plumes,” Doctoral dissertation, Swiss Federal Institute of Technology, ETH Diss. No. 14799, Zurich, Switzerland (2002)

[23] J. H. Milgram, “Mean Flow in Round Bubble Plumes,” *J. Fluid Mech.,* **133** (1983) 345–376.

[24] J. Kubasch and G. Yadigaroglu, “Detailed Measurements of Bubble Plume Characteristics in a Large Pool,” Paper No KJ2 in *HEFAT2003, 2nd Int. Conf. On Heat Transfer, Fluid Mechanics and Thermodynamics,* Victoria Fall, Zambia, 23-26 June, 2003.

[25] R. Milenkovic and M. Fehlmann, “Gas-Liquid Injection System (Mass and/or Heat Transfer Apparatus and Method for Mass and/or Heat Transfer Enhancement),” pending *European Patent (No.04008712.4-).*

[26] M. Simiano, R. Zboray, F. de Cachard, D. Lakehal and G. Yadigaroglu, “Extensive Measurements of the Hydrodynamic Characteristics of Large-Scale Bubble Plumes,” P*roc. 5th International Conference on Multiphase Flow, ICMF’04,* Yokohama, Japan, May 30-June 4, 2004, Paper No. 304.

[27] R. Zboray, M. Simiano and F. de Cachard, “Local Two-Phase Flow Measurements with Advanced Data Processing Methods in Bubbly Plumes,” *Proc. 3rd International Symposium on Two-Phase Flow Modelling and Experimentation*, Pisa, Italy, September 22-25, 2004.

[28] M. Simiano, R. Zboray, F. de Cachard, D. Lakehal and G. Yadigaroglu, "Comprehensive Experimental Investigation of the Hydrodynamics of Large-Scale, 3D, Oscillating Bubble Plumes," to appear in *Int. J. Multiphase Flow,* (2006).

[29] M. Simiano, D. Lakehal and G. Yadigaroglu, "Turbulent Transport Mechanisms in Large-Scale Three Dimensional Bubble Plumes. Part I: Simultaneous Bubble Liquid and Relative Velocity Measurements," to be submitted to *Physics of Fluids.*

[30] M. Simiano, D. Lakehal, M. Lance and G. Yadigaroglu, "Turbulent Transport Mechanisms in Large-Scale Three Dimensional Bubble Plumes. Part II: Role of the Large-Scale Motion to the Velocity and Turbulent Field," to be submitted to *Physics of Fluids.*

[31] R. Milenkovic, B. Sigg and G. Yadigaroglu, "Study of Periodically Excited Bubbly Jets by PIV and Double Optical Sensors," *Int. J. Heat and Fluid Flow,* **26** (2005) 922-930.

[32] R. Milenkovic, B. Sigg and G. Yadigaroglu, "Excited Single-Phase (Liquid) Jets," *J. of Visualization,* **8** (2005) 289.

[33] M. Milelli, B.L. Smith, D. Lakehal, "Large Eddy Simulation of Turbulent Shear Flows Laden with Bubbles," in *Direct and Large-Eddy Simulation - IV,* ERCOFTAC Series, 8, pp. 461-470, Geurts/Friedrich/Metais (Eds.), Kluwer Acad. 2001.

[34] M. Milelli, B.L. Smith, D. Lakehal, "Subgrid Scale Modelling in LES of Turbulent Bubbly Flows," *Proc. Turbulent Shear Flows & Phenomena 2*, Stockholm, June 27-29, 2001, Vol. II, pp. 181-186, Lindborg/Johansson/Eaton (Eds.).

[35] D. Lakehal, B.L. Smith and M. Milelli, "Large-Eddy Simulation of Bubbly Turbulent Shear Flows," *Journal of Turbulence,* **3(25)** 1-21 (2002).

[36] P. Liovic , D. Lakehal, "Interface-Turbulence Interactions in Large-Scale Bubbling Processes", *Int. J. Heat and Fluid Flow*, **27**(5), 18 (2006)

[37] P. Liovic, D. Lakehal, "Multi-Physics Treatment in the Vicinity of Arbitrarily Deformable Fluid-Fluid Interfaces", *J. Comp. Physics*, 32 (2006).

[38] M. Meier, "Numerical and Experimental Study of Large Steam/Air Bubbles Condensing in Water". Doctoral Dissertation, Swiss Federal Instsitute of Technology, ETH Diss. No. 13091 (1999).